Thermal Conductivity in Thin Silicon Nanowires: Phonon Confinement Effect

ARTICLE *in* NANO LETTERS · MAY 2007

Impact Factor: 13.59 · DOI: 10.1021/nl062823d · Source: PubMed

NANO LETTERS

2007
Vol. 7, No. 5
1155−1159

Thermal Conductivity in Thin Silicon Nanowires: Phonon Confinement Effect

Inna Ponomareva

Department of Physics, University of Arkansas, Fayetteville, Arkansas 72701

Deepak Srivastava

Advanced Aerospace Materials and Devices, NASA Ames Research Center, MS 229-1, Moffett Field, California 94035-1000

Madhu Menon*

Department of Physics and Astronomy and Center for Computational Sciences, University of Kentucky, Lexington, Kentucky 40506

Received December 3, 2006; Revised Manuscript Received February 13, 2007

ABSTRACT

Thermal conductivity of thin silicon nanowires (1.4–8.3 nm) including the realistic crystalline structures and surface reconstruction effects is investigated using direct molecular dynamics simulations with Stillinger–Weber potential for Si–Si interactions. Thermal conductivity as a function of decreasing nanowire diameter shows an expected decrease due to increased surface scattering effects. However, at very small diameter (<1.5 nm), an increase in the thermal conductivity is observed, which is explained by the phonon confinement effect.

The current surge in interest in silicon nanowires is fueled by their significant potential in various technological applications such as nanoelectronic, electromechanical, mechanical, and thermoelectric devices. In particular, their thermal conductivity is of great interest for their potential application in nanoscale thermoelectric power generators or coolers. The thermal conductivity of thin Si nanowires could deviate substantially from the bulk value due to the larger surface to volume ratio and explicit surface reconstruction effects which could lead possibly to phonon scattering and confinement, especially at small diameters.

Due to the size effect and high surface to volume ratio, the thermal conduction properties of silicon nanostructures differ substantially from those of bulk materials.[1] For very thin silicon films and other nanostructures, the thermal conductivity models have indicated that phonon confinement effects could alter thermal conduction by altering phonon spectra of the materials.[2] Experimentally, it has been found that thermal conductivity of individual silicon nanowires is more than 2 orders of magnitude lower than the bulk value and exhibits strong diameter dependence.[3] Molecular dynamic simulations using the Green−Kubo method have also reported a significant reduction of thermal conductivity in silicon nanowires of square cross sections as compared to that of the thermal conductivity in bulk silicon.[4] The Monte Carlo simulation technique has also been utilized to predict the thermal conductivity of silicon nanowires.[5] Other theoretical results on thermal conductivity of tetrahedral silicon nanowires have also been reported,[6−8] though the diameters of the nanowires simulated were generally larger than 15 nm.

At smaller diameters, however, the surface to volume ratio and the effect of surface reconstruction on the underlying crystalline structures become increasingly dominant and could have a significant effect on the conduction properties. None of the modeling and simulation studies of the thermal conductivity of Si nanowires reported above[4−8] have included consideration of realistic crystalline structures, reconstructed surfaces, and longer lengths in the direct simulations. Using Stillinger−Weber (SW) and generalized tight-binding molecular dynamics (GTBMD) simulations, we have recently investigated structural and mechanical properties of thin Si nanowires with single- and poly-crystalline tetrahedral and cage-like or clathrate-type crystal structures with realistic surface reconstruction in all of the cases for diameters varying between 1 and 5 nm.[9,10] The diamond like tetrahedral and cage like clathrate lattice structures with realistic surface reconstruction were found to be the most stable structures as compared to the polycrystalline structures in all diameter ranges.[10]

* To whom correspondence should be addressed. E-mail: super250@pop.uky.edu.

10.1021/nl062823d CCC: $37.00
Published on Web 03/30/2007

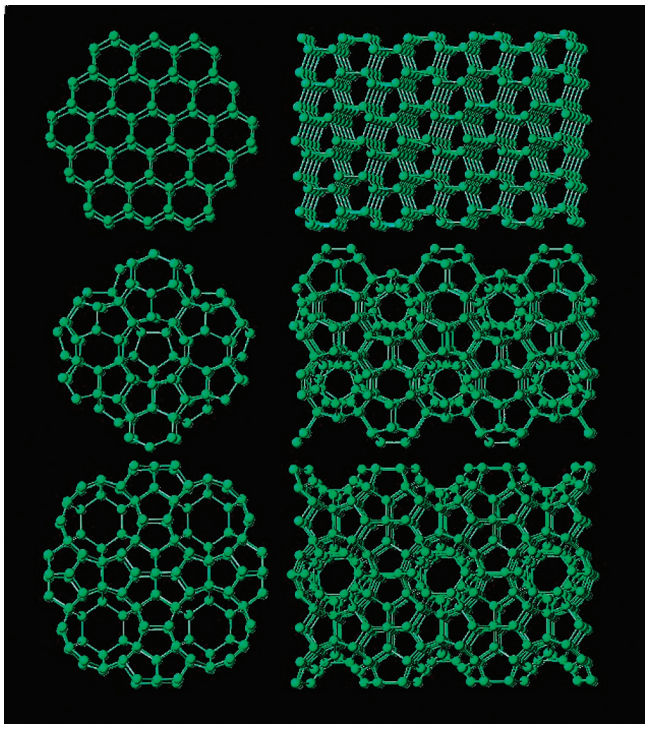

Figure 1. Representative from each fully relaxed silicon nanowires considered in the present work with cores consisting of tetrahedral (top), Si_{34} clathrate (middle), and Si_{46} clathrate (bottom) structures.

In this work, we focus on the thermal conductivity of three different types of silicon nanowires, namely the tetrahedral wires oriented along the [111] direction and clathrate wires represented by Si_{34} and Si_{46} clathrate structures, with diameters in the range of 1.4−8.3 nm and realistic surface reconstruction in all cases. The bulk Si_{34} clathrate structure consists of a face centered cubic (fcc) lattice with a 34 atom basis, whereas the bulk Si_{46} clathrate structure consists of a a simple cubic (sc) lattice with a 46 atom basis.[10] The clathrate nanowires are obtained by carving out cylindrical portions from these crystalline structures. All of the nanowire structures were fully relaxed using molecular dynamics simulations with the SW many body potential[11] allowing for realistic surface reconstruction. By latter we mean that all of the surface Si atoms rearrange to minimize their surface energy and have 3-fold coordination instead of the usual 2-fold surface coordination if the surface is directly cut from the bulk material. Figure 1 shows a representative each from the three different types of nanowires considered in the present work.

The thermal conductivity is calculated using the direct method[12] and is analogous to the experimental method. This method requires the use of nonequilibrium molecular dynamics (NEMD) and is known to provide good results for bulk silicon.[12] The Si−Si interaction potential used in the MD simulations is taken to be the SW many-body potential.[11] The SW interatomic potential consists of two- and three-body interaction terms and was originally fitted to describe correctly the crystalline and liquid phases of bulk silicon. This potential has been used in the study of molten Si,[11] surfaces of crystalline Si,[13] and recently in the structure and nanomechanics of thin Si nanowires.[9,10] The bulk values of thermal conductivity obtained with SW potential in the framework of the direct (nonequilibrium molecular dynamics) method are 119 ± 40 W/mK at $T = 500$ K and 65 ± 16 W/mK at $T = 1000$ K. The corresponding extrapolated experimental values for isotropically enriched Si are 120 and 50 W/mK, respectively.[12]

The super cell used in the calculation of thermal conductivity is divided into N slabs along the direction of the measurement (z axis in our case). One of these slabs is used as the heat source, and another is used as the heat sink.[14] Each particle velocity in the source/sink region is scaled by the same factor so that the resulting kinetic energy is increased/decreased by an amount $\Delta\epsilon$. When the system achieves steady state, the heat current along the z direction is given by $J_z = \Delta\epsilon/2A\Delta t$, where A is the cross section of the wire and Δt is the time step (0.383 fs in our simulations). The resulting temperature gradient along the z axis ($\partial T/\partial z$) is then calculated and Fourier's law is used to obtain thermal conductivity k according to

$$J_z = \frac{-k\partial T}{\partial z} \tag{1}$$

We have used $\Delta\epsilon = 4.3 \times 10^{-4}$ eV which seems to be an appropriate choice for the nanowire cross sections used in our simulations.[12] We have used the velocity-rescaling algorithm of Jund and Jullien[15] to eliminate the tendency of the center of mass of the entire system to drift.

To determine the optimal length of the super cell along the z direction, we conducted a series of simulations for tetrahedral nanowires of diameter 4.2 nm with super cell lengths of 75, 100, and 125 nm. The temperature profiles resulting from these simulations are shown in Figure 2. It can be seen from this figure that the super cell length of 100 nm is long enough to achieve a good convergence with respect to the super cell length. This super cell of tetrahedral (clathrate) wires was divided into 80 (100) identical slabs along the z direction. We have chosen different numbers of slabs for tetrahedral and clathrate wires to keep the number of atoms per slab comparable to each other between two type of wires. The 21st (26th) and 61st (76th) slabs were used, respectively, as the sink and source for tetrahedral (clathrate) type wires. From Figure 2, it can also be seen that after the first 76.6 ps of simulation time the temperature gradient does not change substantially. On this basis, we performed all further simulations for 306.4 ps, and the results of the second, third, and fourth simulation periods (153.2, 229.8, and 306.4 ps, respectively) were used for the calculation of the average temperature gradient.

We first study thermal conductivity as a function of temperature for nanowires of similar diameters (4.2, 4.2, and 4.4 nm for tetrahedral as well as Si_{46} and Si_{34} clathrate nanowires, respectively). The dependence of thermal conductivity on the temperature of these nanowires is shown in Figure 3 (top). For the tetrahedral wire, there is a maximum in the thermal conductivity between 100 and 200 K which is in agreement with experimental results for individual Si nanowires.[3] This should be contrasted with the peak of bulk

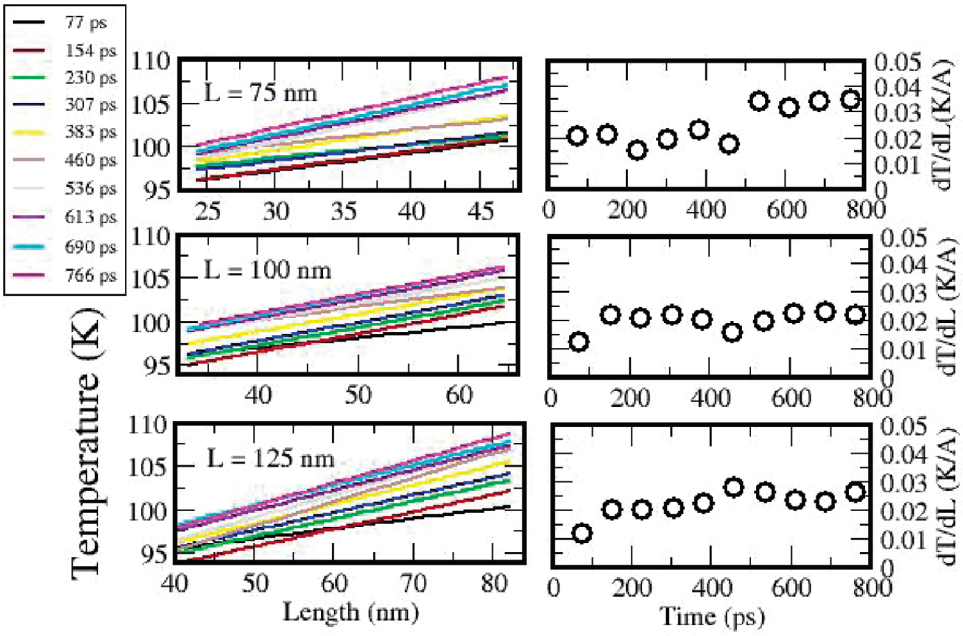

Figure 2. Convergence of temperature gradient at $T = 100$ K for a tetrahedral wire of 4.2 nm in diameter with respect to simulation time and super cell length. First, second, and third rows of the figure show simulation results for super cell lengths 75, 100, and 125 nm, respectively. The first column shows the temperature gradient obtained in the simulation for different simulation time (shown in different colors) after liner interpolation. The last column shows the temperature gradient as a function of simulation time.

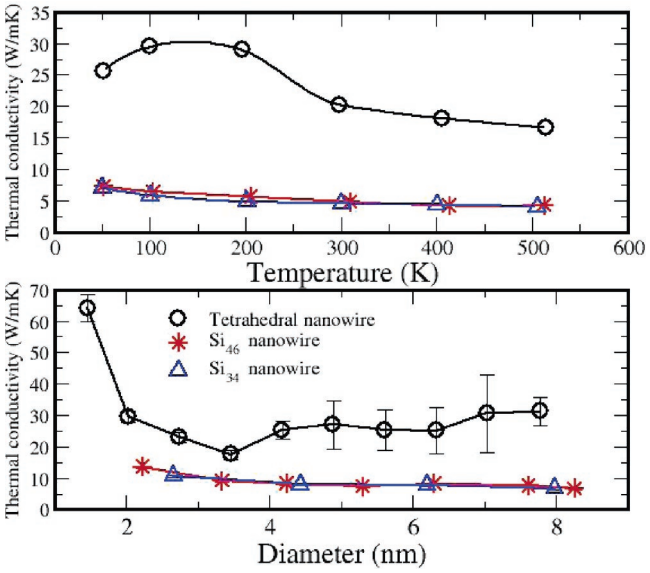

Figure 3. (Top) Thermal conductivity as a function of temperature for different type nanowires of ≈4 nm in diameter. (Bottom) Thermal conductivity at $T = 100$ K as a function of diameter for different type nanowires.

Si that occurs at about 25 K. The peak in bulk silicon is related to boundary scattering, depends on the sample size, and is not directly related to the maximum observed in the nanowire. Thermal conductivity of clathrate nanowires on the contrary does not exhibit any peak in the temperature range considered here. The magnitude of thermal conductivity of tetrahedral wires is qualitatively in good agreement with experimental data, although direct comparison cannot be made since the nanowires considered here have a much smaller diameter than the experimentally available data. The thermal conductivity of clathrate wires is about 3 times lower than the thermal conductivity of tetrahedral wires. This is in qualitative agreement with the experimental finding that the magnitude of thermal conductivity of guest-free silicon Si_{34} clathrate with the type-II hydrate crystal structure is an order of magnitude less than that of the Si diamond structures.[16]

The diameter dependence of the thermal conductivity of silicon nanowires calculated at $T = 100$ K, since all of the nanowires have relatively high thermal conductivity at this temperature, is described next. Thermal conductivity as a function of diameter for various nanowires is shown in Figure 3 (bottom). The thermal conductivity of tetrahedral wires decreases with the wire diameter decreasing from 7.7 to 3.4 nm. As mentioned above, this behavior is consistent with the experimental findings[3] and can be attributed to the increase in surface to volume ratio resulting in the surface scattering of the relevant phonons and a reduction in the thermal conductivity. A striking feature is seen, however, as the nanowire diameter continues to decrease further; the thermal conductivity starts to increase again. A similar behavior in the increase in the thermal conductivity of clathrate nanowires with decreasing diameter is observed, but the magnitude is much smaller. The thermal conductivity for the smallest diameter clathrate nanowire is relatively high and decreases as the nanowire diameter increases for up to 8.2 nm. The overall decrease is much smaller than the decrease in the case of diamond like tetrahedral nanowires; no increase in the thermal conductivity for up to 8.2 nm diameter nanowire is observed. We expect that the thermal conductivity for clathrate nanowires may increase for even larger diameters, which are beyond the scope of the current simulation work.

To account for this striking confinement induced increase in the thermal conductivity for the smallest (≈ 1 nm)

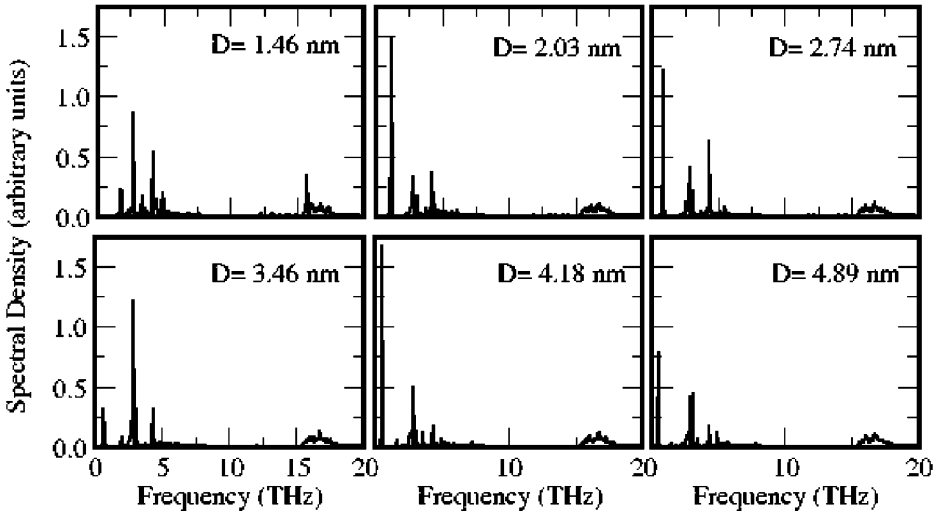

Figure 4. Spectral densities of different diameter tetrahedral nanowires calculated at $T = 100$ K.

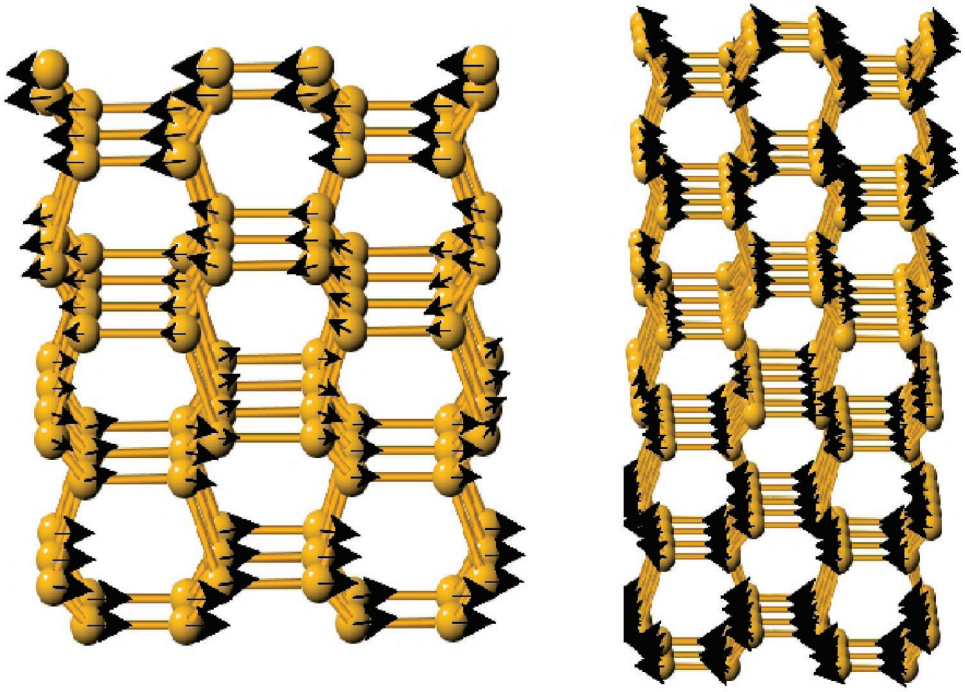

Figure 5. Schematic representation of the lowest frequency mode for the two smallest diameter tetrahedral nanowires. The figure shows the side view for each.

diameter nanowires, the low temperature (100 K) phonon spectra or density of states was computed as a function of nanowire diameter. The phonon spectra were computed by taking the Fourier transform of the velocity autocorrelation function on the data at 100 K after an equilibrium was achieved. The velocity autocorrelation functions were calculated with a simulation run over 27.0 ps with the average taken over 500 simulations with the technique recently suggested.[17] The spectral densities of tetrahedral wires for up to 4.9 nm diameter are shown in Figure 4. The frequencies of the main peaks are given in Table 1.

The long wavelength and low frequency (0−5 THz) region of the phonon spectral density was analyzed for confinement effects. The most prominent low frequency and long wavelength modes that show significant excitation at 100 K are listed in Table 1. As the diameter of the nanowire decreases, the lowest frequency and longest wavelength excited mode is affected the most and shows the signature of confinement. As the nanowire diameter decreases from 5 to 1.4 nm, the frequency of this mode increases from 0.5 to 1.78 THz (an increase by a factor of ≈3.5), respectively. This mode is shown schematically in Figure 5 for the two smallest diameter tetrahedral nanowires considered in the present work. The frequency of the next significant mode decreases from 2.9 to 2.7 THz (a decrease by only a factor of 6%). The confinement induced increase in the frequency of the excited longest wavelength phonon in the spectra thus dominates the changes in the spectra in the low frequency

Table 1. Frequency Peaks of Si-NWs for Various Diameters

wire	diameter (nm)	frequency peaks (THz)
tetrahedral	1.4	1.78, 2.70, 3.35, 4.15, 4.90, 15.44−18.2
tetrahedral	2.0	1.19, 2.82, 3.14, 4.25, 15.44−18.2
tetrahedral	2.7	0.89, 2.86,3.09, 4.35, 15.44−18.2
tetrahedral	3.5	0.70, 2.87, 3.04, 4.35, 15.44−18.2
tetrahedral	4.2	0.60, 2.89, 3.04, 4.40, 15.44−18.2
tetrahedral	5.0	0.51, 2.89, 3.09, 4.34, 4.9, 15.44−18.2
Si_{34}	2.7	1.0−9.02, 14.0, 14.1, 16.3, 16.7, 17.1
Si_{34}	4.4	1.0−8.9,14.0,14.3,16.2,16.7,16.9,17.2
Si_{34}	6.3	1.0−9.0, 14.0,14.4, 16.2, 16.7, 16.9,17.2
Si_{46}	2.2	1.0−9.0, 14.07,14.3, 15.04,16.0, 16.5,17.0
Si_{46}	3.3	1.0−9.0, 14.2, 15.1, 15.9−17.1
Si_{46}	3.3	1.0−9.0, 14.2, 15.0, 15.9−17.1

or long wavelength region resulting in a larger amount of energy carried by the longest wavelength phonon and an increase in the thermal conductivity for the smallest diameter nanowire.

It should be noted, however, that for a fixed thermal gradient the thermal conductivity is directly proportional to the heat current flux through the nanowire. The latter derives its contributions not only from the different phonon modes but also from other factors; namely, the distribution of modes, group velocity, and phonon−phonon scattering effects. Since only the lowest excited phonon mode shows the confinement effect, the group velocity, mode distribution, and phonon-scattering effects are not expected to change appreciably with the nanowire diameter. The thermal conductivity increase at low temperatures, therefore, can be attributed mainly to the increase in the frequency of the lowest mode with decreasing diameter. There is also another point worth noting. Although the predicted increase of thermal conductivity for small diameter nanowires is expected to be significant at low temperatures, such behavior might be different at higher temperatures. This is because, as temperature increases, the broadening in the peaks of spectral distribution function may result in the coupling between the neighboring modes, reducing the relative contribution of the confined mode to the increase in the overall thermal conductivity.

In summary, the thermal conductivity of thin Si nanowires of tetrahedral and clathrate-type lattice structures with realistic relaxed crystal structures and surface reconstructions has been computed and analyzed as a function of nanowire diameter. For the smallest diameter (1.4 nm) tetrahedral nanowires, we observe and analyze the confinement induced increase in thermal conductivity and identify the phonon responsible for this effect in the thermal transport behavior.

Acknowledgment. The present work is supported through grants by NSF (ITR-0221916), DOE (DE-FG02-00ER45817), and US-ARO (W911NF-05−1-0372). Part of this work (DS) is supported by NASA Contract NAS2−03144 to UARC. D.S. also thanks Dr. Natalio Mingo for valuable discussions during this work.

References

(1) McConnell, A.; Goodson, K. *Ann. Rev. Heat Transfer* **2005**, *14*; Chapter II.3.
(2) Balandin, A.; Wang, K. *Phys. Rev. B* **1998**, *58*, 1544.
(3) Li, D.; Wu, Y.; Kim, P.; Shi, L.; Yang, P.; Majumdar, A. *Appl. Phys. Lett.* **2003**, *83*, 2934.
(4) Volz, S.; Chen, G. *Appl. Phys. Lett.* **1999**, *75*, 2056.
(5) Chen, Y.; Li, D.; Lukes, J.; Majumdar, A. *J. Heat Transfer*. **1999**, *127*, 1129.
(6) Mingo, N. *Phys. Rev. B* **2003**, *68*, 113308.
(7) Mingo, N.; Yang, L.; Li, D.; Majumdar, A. *Nano Lett*. **2003**, *3*, 1713.
(8) Lu, X.; Chu, J.; Shen, W. *J. Appl. Phys.* **2003**, *93*, 1219.
(9) Menon, M.; Srivastava, D.; Ponomareva, I.; Chernozatonskii, L. A. *Phys. Rev. B* **2004**, *70*, 12.
(10) Ponomareva, I.; Menon, M.; Srivastava, D.; Andriotis, A. N. *Phys. Rev. Lett.* **2005**, *95*, 265502.
(11) Stillinger, F.; Weber, T. *Phys. Rev. B* **1985**, *31*, 5262.
(12) Schelling, P.; Phillpot, S.; Keblinski, P. *Phys. Rev. B* **2002**, *65*, 144306.
(13) Abraham, F. F.; Batra, I. P. *Surf. Sci.* **1985**, *163*, L752.
(14) See ref 12 for details of the setup.
(15) Jund, P.; Jullien, R. *Phys. Rev. B* **1999**, *59*, 13707.
(16) Nolas, G.; Beekman, M.; Gryko, J.; Lemberton, G., Jr.; Tritt, T.; McMillan, P. *Appl. Phys. Lett.* **2003**, *82*, 910.
(17) Rapaport, D. *The Art of Molecular Dynamics Simulation*; Cambridge University Press: New York, 2001; Chapter 5.

NL062823D